9-2021

Laser-Defined Graphene Strain Sensor Directly Fabricated on 3D-Printed Structure

Tyler M. Webb
Boise State University

Twinkle Pandhi
Boise State University

David Estrada
Boise State University

Publication Information

Aga, Robert S.; Webb, Tyler M.; Pandhi, Twinkle; Aga, Rachel; Estrada, David; Burzynski, Katherine M.; . . . and Heckman, Emily M. (2021). "Laser-Defined Graphene Strain Sensor Directly Fabricated on 3D-Printed Structure". *Flexible and Printed Electronics, 6*(3), 032001. https://doi.org/10.1088/2058-8585/abf0f8

Laser-defined graphene strain sensor directly fabricated on 3D-printed structure

Roberto S. Aga[1], Tyler M. Webb[2], Twinkle Pandhi[2], Rachel Aga[3], David Estrada[2], Carrie M. Bartsch[4] and Emily M. Heckman[4]

[1] KBR, 2601 Mission Point Blvd, Suite 300, Dayton, OH 45431, USA
[2] Micron School of Materials Science and Engineering, Boise State University, Boise, ID 83725, USA
[3] Department of Chemistry, Wright State University, Dayton, OH 45435, USA
[4] Air Force Research Laboratory, Sensors Directorate, 2241 Avionics Circle, WPAFB, OH 45433

E-mail: Roberto.Aga@us.kbr.com

Abstract

A direct-write method to fabricate a strain sensor directly on a structure of interest is reported. In this method, a commercial graphene ink is printed as a square patch (6 mm square) on the structure. The patch is dried at 100 °C for 30 min to remove residual solvents but the printed graphene remains in an insulative state. By scanning a focused laser (830 nm, 100 mW), the graphene becomes electrically conductive and exhibits a piezoresistive effect and a low temperature coefficient of resistance (*TCR*) of -0.0006/°C. Using this approach, the laser defines a strain sensor pattern on the printed graphene patch. To demonstrate the method, a strain sensor was directly fabricated on a 3D-printed test coupon made of ULTEM 9085 thermoplastic. The sensor exhibits a gauge factor of 3.58, which is significantly higher than that of commercial foil strain gauges made of constantan. This method is an attractive alternative when commercial strain sensors are difficult to employ due to the high porosity and surface roughness of the material structure under test.

Keywords: strain sensor, graphene, printed electronics, additive manufacturing

1. Introduction

Strain sensors are widely used in the fields of healthcare, structural health monitoring, automotive and aerospace. Examples of their applications include wearable devices for detection of human activities [1], monitoring structural integrity of bridges [2] and material testing for automotive and aerospace engines [3]. The development of strain sensors is still a very active area of research despite their commercial availability. This is primarily motivated by the limitation of commercial sensors, which typically require careful bonding and surface preparation to the material structure of interest. Their packaging and form factor may also be incompatible with certain applications such as for human wearables. This presents a need to embed strain sensors in unconventional materials such as textiles [4].

3D-printed materials continue to gain attention as alternatives for structural applications. They have been explored for the fabrication of small unmanned aerial vehicles (UAVs) [5] and motors for wind energy harvesting [6]. Similar to their conventional counterparts, they require comprehensive mechanical testing before widespread use. Additionally, their structural health may need to be monitored while deployed. Mechanical testing and structural monitoring often involve strain sensors. However, some 3D-printed materials have inherently high porosity and high surface roughness, often making it difficult to attach a commercial strain gauge (COTS-SG). An example of such a material is the ULTEM material series, a thermoplastic that can be 3D-printed by fused deposition modelling (FDM) printers. It is promising for structural applications due to its mechanical strength and high thermal stability. For ULTEM 1010, the glass transition temperature is 215 °C. Attaching COTS-SG on ULTEM is a

challenge because it requires special adhesives and careful surface preparation [7]. Due to the porous nature of ULTEM, the adhesive fills the voids and consequently modifies the mechanical property of the region underneath the COTS-SG, which can compromise the strain measurements.

Graphene-based nanomaterials have recently been explored for strain sensing applications because of its high mechanical strength and excellent mechanical flexibility that allow it to tolerate high strain levels [8]. Moreover, the electrical resistance of graphene does not change significantly over a wide temperature range, which is a desirable property for strain sensors. Additionally, with the emergence of commercially available graphene ink, graphene-based devices can be fabricated using additive manufacturing. In this work, the issues of COTS-SG are addressed by using graphene ink and additive manufacturing to fabricate a strain sensor directly on a 3D-printed thermoplastic structure that is porous and has high surface roughness. This recently patented technique circumvents the problems associated with attaching COTS-SG on unconventional surfaces such as that of 3D-printed ULTEM [9]. Unlike other printed graphene strain sensors [10], the technique reported here relies on a laser sintering tool to define the strain gauge pattern, rather than the printer itself, thereby eliminating the need for a high-precision printing tool.

2. Experiment

Graphene ink was purchased from Sigma-Aldrich (#798983-10ML) and used as received. It was printed with an NSCRYPT Tabletop 3Dn extrusion printer. After printing, laser sintering in ambient air was used to make the printed graphene electrically conductive. A laser with wavelength of 830 nm equipped with 10X focusing objective lens was used. Incident optical power and scanning speed were optimized to obtain the lowest electrical resistance of the printed graphene then the electrical resistivity (ρ), temperature coefficient of resistance (*TCR*) and work function of the laser-sintered graphene were measured. They were compared to their thermally annealed counterpart. Measurement of ρ was performed on traces printed on a glass substrate using a four-point probe method [11]. In this method, the ρ value is calculated from the measured resistance R of the trace of length L and cross section area ϕ as given by equation 1 below:

$$\rho = \frac{\phi R}{L} \qquad [1]$$

The cross sectional area was measured by stylus profilometry using a Dektak XT. The *TCR* was determined using the same sample for the ρ measurement. The trace resistance R was measured in a nitrogen environment at different temperatures T from 21 °C to 100 °C. The average *TCR* in that temperature range was extracted from the plot of R versus T. The work function was measured using a Kelvin probe as described in a previous publication [12].

The laser-defined graphene strain sensor (LD-GSS) was directly fabricated on a 3D-printed thermoplastic coupon made of ULTEM 9085. The coupon, with a dimension of 127 mm x 38 mm and thickness of 1.3 mm, was printed by a Fortus 450mc from Stratasys. Fig. 1(a) illustrates the two main steps in the fabrication process. The graphene is first printed as a square patch (6 mm^2) on the coupon and it is dried on a hotplate at 120 °C for 30 min. After drying, the strain sensor pattern is created on the graphene patch by scanning the focused laser beam in a controlled manner. The sensor pattern consists of two adjacent traces parallel to the longer side of the coupon, which is designated as the x-axis. The two traces are electrically connected by a connecting pad at one end. At the other end, each trace is terminated by two separate pads, which serve as contact pads for the wire leads to the sensor. AWG 40 copper wires were used as the wire leads. They were attached to the contact pads using a conductive silver adhesive from Creative Materials (#118-15). The adhesive was cured by baking the coupon on a hotplate at 120 °C for 20 min.

To test the LD-GSS, a cantilever beam method was employed. In this method, the ULTEM coupon functions as a cantilever. Strain ε is applied by bending the coupon as demonstrated in Fig. 1(b). One end of the coupon is constrained by clamping it while the other end is free to move in the vertical direction. The free end is attached to a caliper

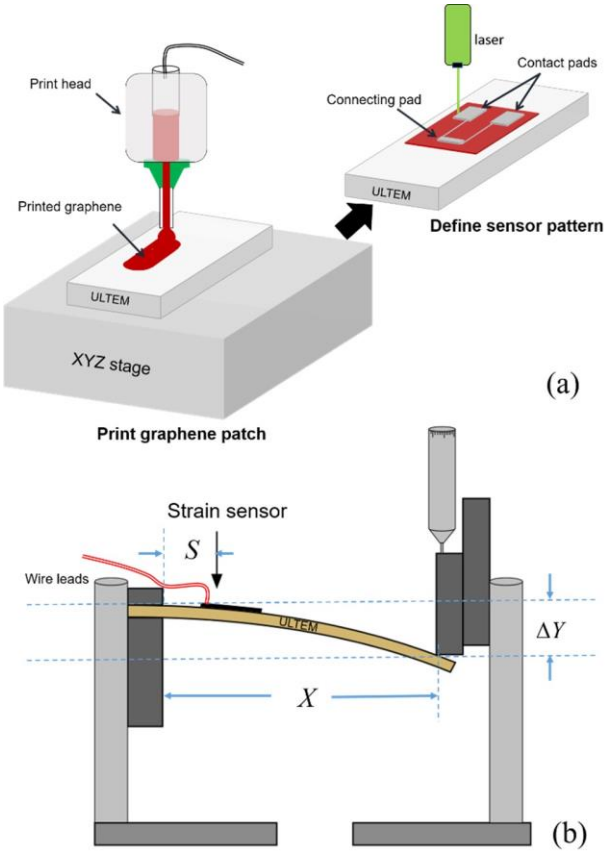

Figure 1. (a) Two-step process of fabricating strain sensor directly on 3D-printed ULTEM. (b) Experimental setup for measuring gauge factor.

to quantify its vertical displacement (ΔY) with respect to the unbent condition. The maximum ΔY of the caliper is 25 mm with a resolution of 10 μm. The distance of the LD-GSS from the constrained end is given by *S*. The point on the coupon where the caliper exerts a downward force for bending has a distance of *X* from the constrained end. If the values of *S* and *X* are known, the value of ε at the location of the LD-GSS for a specific ΔY can be calculated. The calculation was performed using the COMSOL Multiphysics software package. Since *S* and *X* were fixed in the experiment, the exact relationship between ε and ΔY was determined.

The relative change in resistance of the LD-GSS due to ε was defined as $\Delta R/R_o$ where R_o is the resistance when $\varepsilon = 0$ (unbent condition). It was measured at the wire leads attached to the contact pads using a lock-in technique. To briefly describe the measurement, a 1 kHz sinusoidal voltage from a function generator (Stanford Research DS345) is applied to the LD-GSS via a 25 MΩ series resistor. The voltage across the LD-GSS is measured by a lock-in amplifier (Stanford Research SR530) with the 1 kHz sinusoidal voltage from the function generator as the reference. The amplitude of the applied voltage is set to give a lock-in reading of 400±5 μV when $\varepsilon = 0$. This voltage value is defined as V_o. When ε is applied, the change in voltage with respect to V_o is measured and defined as ΔV. The ratio $\Delta V/V_o$ provides the value of $\Delta R/R_o$. The sensitivity of the lock-in amplifier was set to measure a maximum voltage of 500 μV. With this setting, the smallest $\Delta R/R_o$ that could be detected was $5\text{x}10^{-4}$. To obtain the gauge factor (*GF*) of the LD-GSS, $\Delta R/R_o$ was measured and plotted as a function of ε. The value of ε was varied by bending the cantilever from $\Delta Y = 0$ to 25 mm at 2.5 mm increment. The slope of the plot was extracted to give the *GF* value. To validate the experimental method, a commercial foil strain gauge with known *GF* from Omega (#KFH-3-350-C1-11L1M2R) was also tested. It was glued on a Rogers RO4053B PCB board with the same dimension as the ULTEM coupon.

3. Results and Discussion

The commercial graphene ink remains an insulator after printing and requires post-print sintering to become electrically conductive. The vendor recommends thermal sintering at 300 °C for 30 min for a film thickness >100 nm. Using this condition, the measured ρ of the printed graphene trace was 0.007 Ω-cm and is within the range of ρ provided by the vendor. Another alternative to thermal sintering is laser sintering. It was found that for a laser wavelength of 830 nm, incident power of 100 mW and a scanning speed of 2.5 mm/s, a ρ of 0.011Ω-cm was achieved. While the ρ of laser-sintered graphene trace was observed to be slightly higher as compared to its thermally sintered counterpart, it was still within the range that is suitable for piezoresistive-based sensing. This is a similar result as to what has been observed in printed silver nanoparticle ink; laser sintering of silver nanoparticle ink typically yields higher ρ as compared to thermal sintering because it increases porosity [13]. The behavior of graphene resistance *R* with temperature *T* was the same regardless of sintering method employed and no difference in the *TCR* was detected between the two sintering methods. Fig. 2(a) is a typical *R*(*T*) plot of a laser-sintered graphene. It demonstrates that resistance of graphene decreases with increasing temperature. The rate of decrease is fairly linear from 21 °C to 100 °C with an average *TCR* of -0.0006/°C. This is an order of magnitude lower than elemental metals and is desirable for strain sensors to minimize the effect of temperature fluctuation of the environment. It was calculated from equation 2 given below:

$$TCR = \frac{1}{R_{rt}} \frac{dR}{dT} \quad [2]$$

where R_{rt} is the resistance at room temperature (25 °C) and *dR/dT* is the slope of the red line fitted to the *R*(*T*) plot. The work function of laser-sintered and thermal-sintered graphene was observed to be the same at 5.2 eV. This suggests that laser sintering is as effective as thermal annealing in decomposing most of the unwanted ingredients in the graphene ink that hinders electrical conduction. For comparison, the reported work function of very pure graphene is 4.3 eV for a single layer and 4.7 eV for more than 10 layers [14]. This discrepancy is likely due to the presence of other ingredients commonly required in formulating a stable graphene ink.

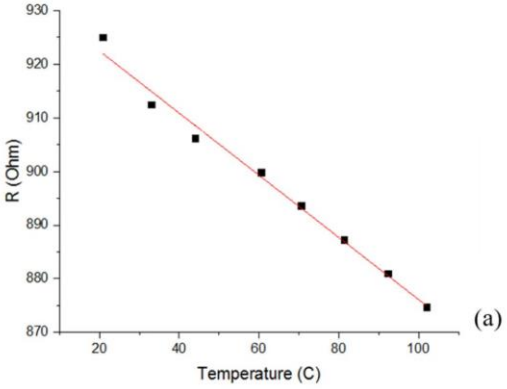

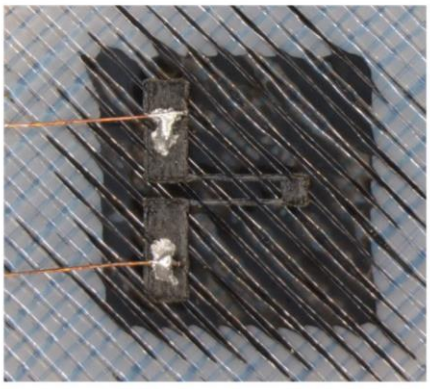

Fig. 2. (a) Resistance of laser-sintered graphene as a function of temperature. (b) Photo of a completed laser-defined graphene strain sensor (LD-GSS) on ULTEM.

In this work, the aim was to print a graphene-based strain sensor on the 3D-printed material ULTEM 9085. While this FDM-printed material has superior mechanical and thermal properties compared to other 3D printed materials, the downside is that it has a fairly large average surface roughness of ~170 μm. This makes it very difficult to achieve the resolution typically required of a strain gauge when printing electrically conductive inks on ULTEM. To address this difficulty, rather than print the strain gauge pattern the graphene was printed as a square patch and the conducting pattern of the strain sensor was defined on the patch by selective laser sintering. The effect of laser sintering is similar to that of thermal annealing; it decomposes the ethyl cellulose that encapsulates the graphene flakes preventing inter-flake charge transport [15]. With selective laser sintering, only the region exposed to the laser beam becomes conducting. If the laser beam is tightly focused, a very fine conducting trace can be created on the patch. Fig. 2(b) is a photo representing a completed LD-GSS with wire leads. It is clearly seen in the photo the high surface roughness of the ULTEM. Due to this roughness, the ink spreads from the edges of the printed graphene patch. However, the poor quality of the edges is not a concern because it does not affect the sensor performance. The crucial part on the patch is the laser-defined conducting pattern, which becomes the piezoresistive strain sensor. The sensor is brighter in color because the printed graphene turns lighter when laser-sintered. It can also be observed in the photo that the sensor has fairly sharp edges. The two fine conducting traces of the sensor, which serve as the strain sensing element, have width and separation of 140 μm and of 500 μm respectively. These results indicate that selective laser sintering is an attractive approach to make tiny graphene-based strain sensors, which may be difficult to print directly on very rough surface. The adhesion of the silver adhesive on the contact pads of the sensor was sufficient to keep the wire leads attached. The contact resistance between the wire and the contact pad was negligible compared to the resistance of the laser-defined conducting pattern. In addition, it did not change with the applied strain. The initial resistance measured at the wire leads of several LD-GSS ranged between 2 to 3 kΩ.

In the experiment, the ULTEM coupon is curved by vertically displacing its free end by ΔY. The curvature stretches the top surface of the coupon inducing a strain parallel to the x direction. Fig. 3(a) maps the strain on the top surface of the coupon as simulated by COMSOL at maximum curvature (ΔY = 25 mm). The level of strain depends on the position along the x direction and it decreases as the position gets farther from the constrained end. The position of the LD-GSS was near the center (S ~ 50 mm). At that position, the strain does not vary significantly along the width of the coupon. The narrow conducting traces of the LD-GSS, which serve as the sensing element, were oriented parallel to the x direction so that they would increase in length (Δl) in response to the curvature. The ratio $\Delta l/l$, where l is the original length, is the strain on the conducting traces. If the conducting traces exhibit piezoresistive effect, their resistance would change due to Δl. Since there is no substrate or adhesive between the LD-GSS and the coupon, the strain on the conducting traces represents very well the strain on the coupon. This is one advantage of LD-GSS over packaged COTS-SG. In the latter, there is a carrier (typically polyimide) and adhesive in between the sensing element and the material under test. Another advantage of the LD-GSS is that it highly conforms to the deformation of the coupon because of the high mechanical flexibility of graphene. It is very important for strain sensors not to oppose the deformation of the material under test and to act as if they are not there at all. Mounting a packaged sensor with adhesive adds more mass that can alter the material property being measured. This is especially true for porous materials such as ULTEM because when the adhesive fills the voids, it can modify the density of the porous material. For the LD-GSS, the penetration of the graphene ink into the voids may have a lesser effect because it consists of nano-flakes that can form a porous film when laser-sintered. To assess the performance of LD-GSS, its gauge factor was measured. Gauge factor is a very important metric of a strain sensor. It is related to $\Delta R/R_o$ and the applied strain ε by equation 3 below:

$$GF = \frac{1}{\varepsilon}\frac{\Delta R}{R_o} \qquad [3]$$

If $\Delta R/R_o$ has a linear dependence on ε, which is usually the case for piezoresistive material, it can be plotted as a function of ε and the slope of the fitted line to the plot represents GF. The value of ε is calculated from equation $\varepsilon = \gamma\,\Delta Y$, where the proportionality constant γ is specific to the position on the coupon. For the position of the LD-GSS (S ~ 50 mm), γ is equal to 1.1 x 10^{-4}/mm from COMSOL simulation. When the measurement procedure was implemented on the COTS-SG,

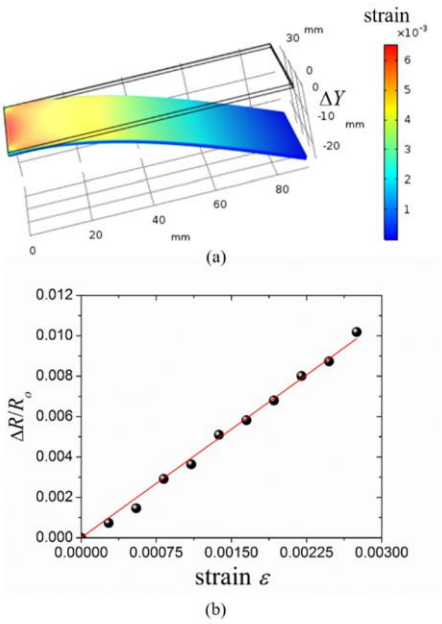

Fig. 3. (a) Simulated map of strain on the ULTEM coupon at maximum vertical displacement of ΔY = 25 mm . (b) Plot of the relative change in resistance $\Delta R/R_o$ of a laser-defined graphene strain sensor (LD-GSS) as a function of applied strain ε.

a *GF* of 1.75 was obtained. The expected *GF* value provided by the manufacturer was 2.0 so the relative percent error in the measurement was 12.5%. The error has two potential sources. The first is from the separation between the sensing element and the surface of the test coupon after mounting the COTS-SG with adhesive. Because of this separation, the strain on the sensing element is always lower than the strain on the coupon. The second source is the discrepancy between the simulated and the actual strain when the coupon is bent. The measurement of *GF* relies on the plot of $\Delta R/R_o$ as a function of ε but the values of ε were simulated and not measured. Measurement of the actual ε on the coupon will improve the experimental method but for the purpose of demonstrating the LD-GSS, it was not necessary. Fig. 3(b) is a representative plot of $\Delta R/R_o$ when ε is incremented from zero to 0.00275. It demonstrates the linear response of the LD-GSS in the range of applied strain. The *GF* of that particular sensor is 3.58 from the slope of the fitted line to the plot. At this stage of development, the *GF* of the sensors can vary from 3.0 to 4.0 but effort is being made to pinpoint the optimum process that yields consistent *GF* and R_o.

4. Conclusion

An alternative method to fabricate a strain sensor directly on a surface was demonstrated on a 3D-printed structure. The method, which uses printable graphene ink, is additive in nature and it is very appropriate for testing and structural health monitoring of materials with high surface roughness and porosity such as thermoplastics created by FDM printers. The graphene is printed as a square patch on the material under test and a conducting pattern, which serves as the piezoresistive strain sensor, is defined by scanning a focused laser. The laser-defined conducting pattern exhibits a *TCR* (temperature coefficient of resistance) of -0.0006/°C. This low value, which is desirable for strain sensing applications, is an order of magnitude lower than that of elemental metals. To demonstrate the proof-of-concept, a strain sensor was directly fabricated on 3D-printed ULTEM, and a gauge factor of 3.58 was achieved. For comparison, the gauge factor of commercial foil strain sensors made of constantan is only 2. The method described here is an attractive option when packaged commercial sensors are difficult to employ or the adhesive required to mount them can alter the mechanical properties of the material under test. It can be extended to directly fabricate strain sensor on a wide range of material structures including non-planar geometries.

References

[1] Guo J, Zhou B 2019 Stretchable and Highly Sensitive Optical Strain Sensors for Human Activity Monitoring and Healthcare *ACS Appl. Mater. Interfaces* 11 33589

[2] Zymelka D, Togashi K and Kobayashi T 2020 Carbon-based printed strain sensor array for remote and automated structural health monitoring *Smart Mater. Struct.* 29 105022

[3] Lei J-F and Will H A 1998 Thin-film thermocouples and strain-gauge technologies for engine applications *Sensors and Actuators A* 65 187

[4] Tian X, Chan K, Hua T, Niu B and Chen S 2020 Wearable strain sensors enabled by integrating one-dimensional polydopamine-enhanced graphene/polyurethane sensing fibers into textile structures *J. Mater. Sci.* 55 17266

[5] Azarov A V, Antonov F K, Golubev M V, Khaziev A R and Ushanov S A 2019 Composite 3D printing for the small size unmanned aerial vehicle structure *Composite Part B.* 169 157

[6] Altan B D, Altan G and Kovan V 2016 Investigation of 3D printed Savonius rotor performance *Renewable Energy* 99 584

[7] https://www.omega.com/en-us/resources/strain-gage-quality-control

[8] Mehmood A, Mubarak N M, Khalid M, Walvekar R, Abdullah E C, Siddiqui M T H, Baloch H A, Nizamuddin S and Mazari S 2020 Graphene based nanomaterials for strain sensor application-a review *J. Environ. Chem. Eng.* 8 103743

[9] Aga R and Heckman E 2020, System and method for fabricating a strain sensing device directly on a structure *US Patent* #10,770,206

[10] Maurya D, Khaleghian S, Sriramdas R, Kumar P, Kishore R A, Kang M G, Kumar V, Song H-C, Lee S-Y, Yan Y, Park J-M, Taheri S and Priya S 2020 3D printed graphene-based self-powered strain sensors for smart tires in autonomous vehicles *Nat. Comm.* 11 5392

[11] Smits F M 1958 Measurement of Sheet Resistivities with the Four-Point Probe *The Bell System Technical Journal* page 711

[12] Aga Jr R, Jordan C, Aga R S, Batsch C M and Heckman E M 2014 Metal Electrode Work Function Modification Using Aerosol Jet Printing *IEEE Elec. Dev. Lett.* 35 1124

[13] Aga R S, Kreit E, Dooley S, Bartsch C M, Heckman E M and Aga R 2018 Considerations in printing conductive traces for high pulsed power applications *Microelectronics Reliability* 81 342

[14] Rut'kov E V, Afana'eva E Y and Gall N R 2020 Graphene and graphite work function depending on layer number on Re *Diamond & Related Materials* 101 107576

[15] Secor E B, Prabhumirashi P L, Puntambekar K, Geier M L and Hersam M C 2013 Inkjet Printing of High Conductivity, Flexible Graphene Patterns *J. Phys. Chem. Lett.* 4 1347